ELECTRONIC SUPPLEMENTARY INFORMATION

Solution-processed In_2Se_3 nanosheets for ultrasensitive and highly selective NO_2 gas sensors

Gianluca D'Olimpio[1,§], Vardan Galstyan[2,3§], Corneliu Ghica[4], Mykhailo Vorokhta[5,] Marian Cosmin Istrate[4], Chia-Nung Kuo[6,7], Chin Shan Lue[6,7], Danil W. Boukhvalov[8,9,*], Elisabetta Comini[2,*], Antonio Politano[1,*]

[1] Department of Physical and Chemical Sciences, University of L'Aquila, via Vetoio, 67100 L'Aquila (AQ), Italy

[2] Sensor Lab, Department of Information Engineering, University of Brescia, Via Valotti 9, 25133 Brescia, Italy

[3] Department of Engineering "Enzo Ferrari", University of Modena and Reggio Emilia, Via Vivarelli 10, 41125 Modena, Italy

[4] National Institute of Materials Physics, Atomistilor 405A, 077125 Magurele, Romania

[5] Charles University, V Holesovickăch 2, Prague 8, 18000 Prague, Czech Republic

[6] Department of Physics, National Cheng Kung University, 1 Ta-Hsueh Road, 70101 Tainan, Taiwan

[7] Taiwan Consortium of Emergent Crystalline Materials, National Science and Technology Council, Taipei 10601, Taiwan

[8] College of Science, Institute of Materials Physics and Chemistry, Nanjing Forestry University, Nanjing 210037, P. R. China

[9] Institute of Physics and Technology, Ural Federal University, Mira 19 Str., Yekaterinburg 620002, Russia

S1. Gas sensing measurements

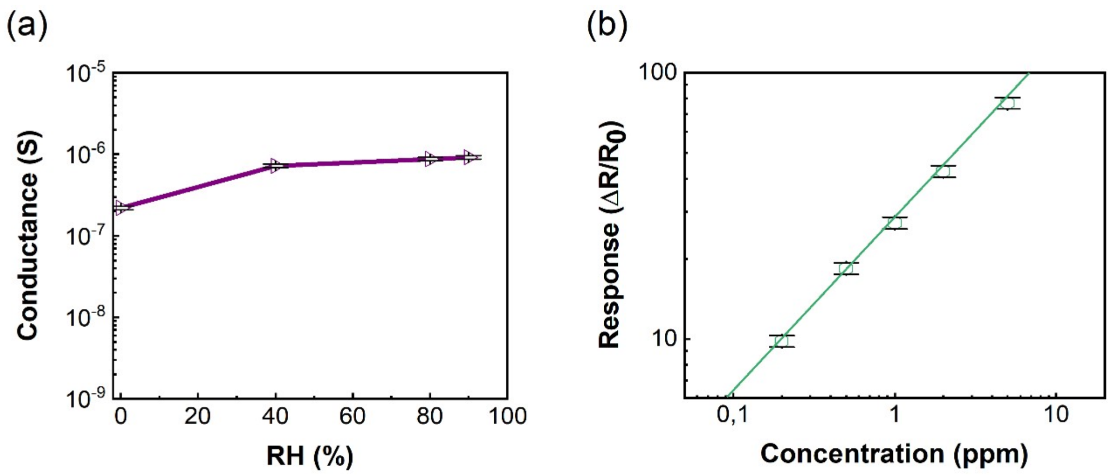

Figure S1. *(a) Electrical conductance dependence of In_2Se_3 on the relative humidity (RH) concentration at an operating temperature of 300 °C. (b) Calibration curve of the normalized sensing response (ΔG/G0) of α-In_2Se_3 towards NO_2 at an operating temperature of 300 °C and RH of 40%. The response value for the pristine structure was set to 1 to estimate the limit of detection (LOD), which was found to be approximately 5 ppb for α-In_2Se_3.*

Table S1. *Gas sensing parameters of In_2Se_3 towards different concentrations of NO_2 at an operating temperature of 300 °C.*

Concentration (ppm)	Response
0.2	9.8
0.5	18.4
1	27.3
2	42.6
5	77.0

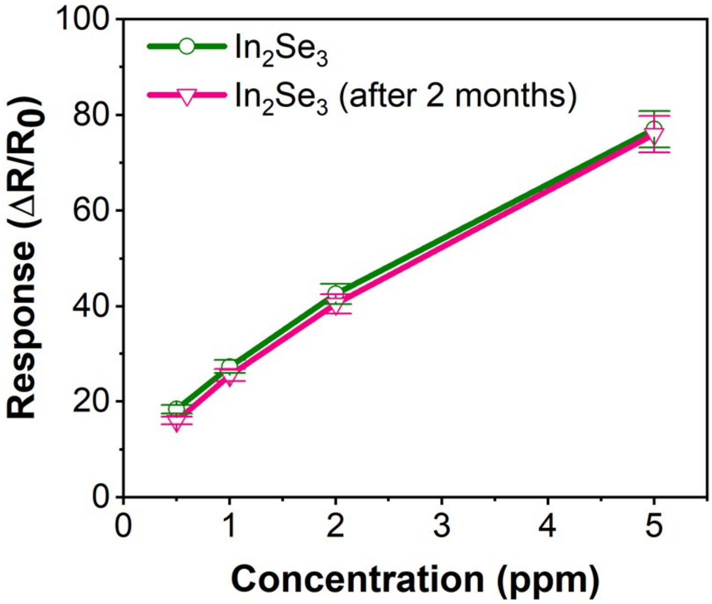

Figure S2. *The response of α-In_2Se_3 towards 0.5, 1, 2, and 5 ppm of NO_2 at its optimum operating temperature (300 °C). The results were obtained after the first-time measurements and two months later.*

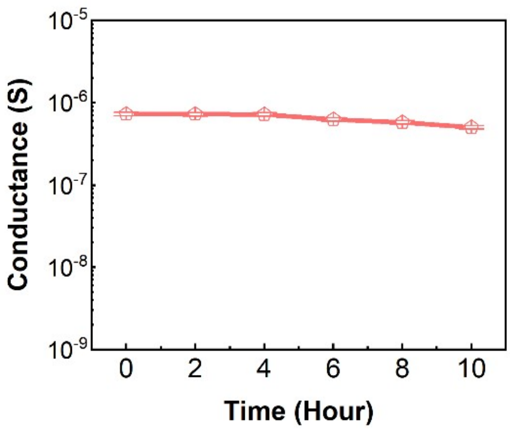

Figure S3. *The conductance vs time dependence of α-In_2Se_3 at 300 °C. The conductance values were registered after the gas test of the material to each concentration of NO_2 (0.2, 0.5, 1, 2, and 5 ppm) and its recovery in air (please see Figure 5b in the paper). The gas test for each concentration of NO_2 lasts 2 h.*

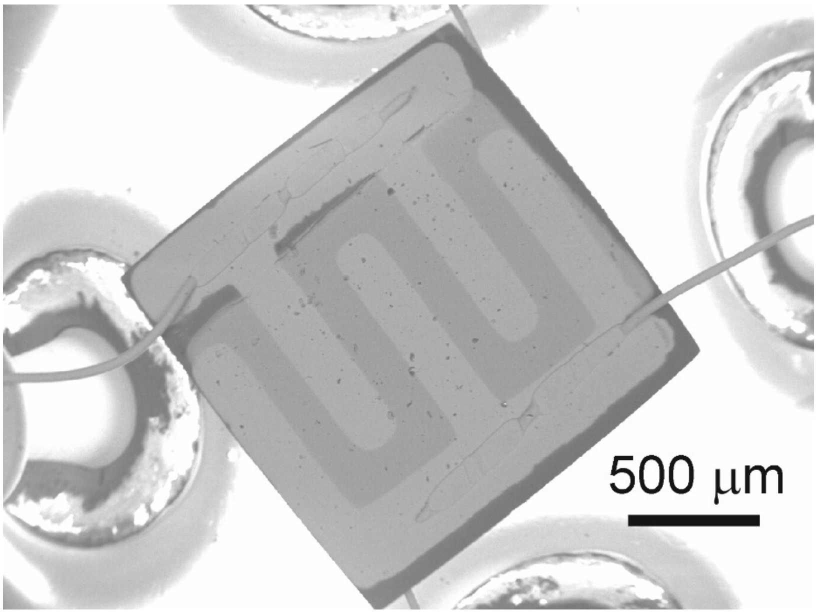

Figure S4. *SEM image of Pt interdigitated electrodes deposited on the Al_2O_3 substrate.*

S2. Literature comparison

Table S2. *Comparison of gas sensing properties of α-In_2Se_3 with sensing structures comprising 2D semiconductors and metal-oxide nanostructures. V_a denotes the output voltage of the sensor in air, while V_g represents the output voltage under exposure to NO_2.*

Material	NO_2 concentration (ppm)	Response $[(R_f-R_0)/R_0]$	Operating temperature (°C)	Estimated LOD (ppb)
SnS_2 [1]	5	2.5	200	–
Sb_2Se_3 [2]	2	0.8, $(R_a-R_g)/R_a$	140	60
N-doped In_2S_3 [3]	10	0.1, $(R_a-R_g)/R_a$	RT	–
$SnO_2/SnSe_{1.7}$ [4]	1	2.2	150	360
In_2O_3/SnS_2 [5]	50	15,* V_g/V_a	25	–
In_2S_3/In_2O_3 [6]	1	24	160	
SnO_2/SnS_2 [7]	3	15.33, R_a/R_g	60	37
$SnSe_2/SnO/SnSe$ [8]	5	2.6	RT	115
reduced graphene oxide [9]	1	0.6,§ $(G_f-G_0)/G_0$	450	50
Black phosphorus	25	0.2	RT	–
Al–Black phosphorus	1	0.1	70	–

10				
reduced graphene oxide/MoS_2 [11]	10	0.1	RT	–
C/g-C_3N_4 [12]	50	0.7	200	7390
In_2O_3 nanoparticles [13]	1.2	0.1, R_a/R_g	300	–
In_2O_3 nanoparticles [14]	40	6, R_a/R_g	225	–
In_2O_3 nanoparticles/SnO_2 nanowires [15]	5	24	300	–
SnO_2 nanowires [15]	5	2.3	300	–
α-In_2Se_3 (this work)	1	27.3	300	5

* Room temperature

§ G_0 is the baseline conductance value of the sensor in air, and G_f is the steady state conductance value of the sensor in presence of NO_2.

S3. O-1s core level measured by XPS

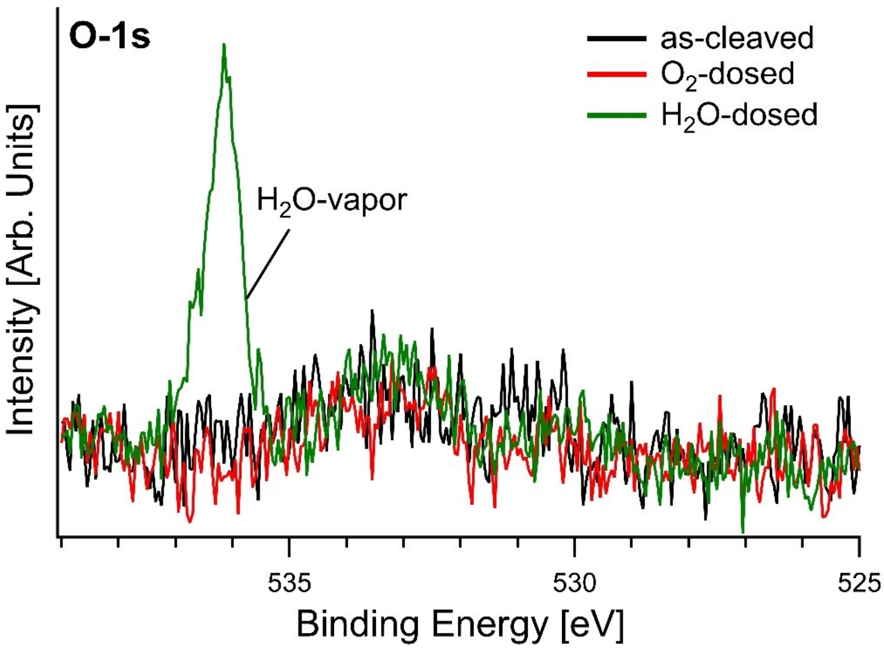

Figure S5. *O-1s core level for the as-cleaved surface of α-In_2Se_3 and for its modification after an exposure of 10^{10} L of O_2 and H_2O at room temperature.*

Table S3. *Differential enthalpy and Gibbs free energies at 400 ºC for the surface of bulk/monolayer of β-In_2Se_3 with and without Se-vacancies. Negative values indicate exothermic processes, while positive values indicate endothermic processes.*

Substrate	Analyte	ΔH, kJ/mol	ΔG (400 ºC), kJ/mol
β-In_2Se_3	O_2	-133.2 / +26.3	-107.3 / +52.2
	H_2	-2.6 / -70.4	+16.1 / -51.7
	H_2O	-296.7 / -61.3	-226.0 / +9.4
	CO	-237.9 / -75.6	-205.6 / -43.3
	CO_2	-289.6 / -78.2	-253.3 / -41.9
	NO_2	-270.2 / -83.4	-214.9 / -8.7
	NO_2+H_2O	+18.7 / -3.8	+93.4 / +70.9
	Ethanol	-306.5 / -95.4	-251.0 / -39.9
	Acetone	-289.7 / -84.1	-216.3 / -10.7
	NH_3	-314.8 / -100.8	-250.9 / -36.9
	H_2S	-302.9 / -86.7	-244.3 / -28.1
β-$In_2Se_{2.97}$	O_2	-4.9 / -56.0	+21.0 / -30.1
	H_2	-17.3 / -8.3	+1.4 / +10.4
	H_2O	-255.9 / -48.2	-185.2 / +22.5
	CO	-53.7 / -37.5	-21.4 / -5.2
	CO_2	-214.0 / -24.3	-177.7 / +12.0
	NO_2	-67.9 / -193.3	+6.8 / -118.6
	Ethanol	-284.8 / -97.0	-229.3 / -41.5
	Acetone	-282.5 / -103.2	-218.4 / -29.8
	NH_3	-291.8 / -84.1	-227.9 / -20.2
	H_2S	-249.4 / -60.2	-190.8 / -1.6

References

1. M. Cheng, Z. Wu, G. Liu, L. Zhao, Y. Gao, B. Zhang, F. Liu, X. Yan, X. Liang, P. Sun and G. Lu, *Sens. Actuators B Chem.*, 2019, **291**, 216-225.
2. Y. B. Kim, S. H. Jung, D. S. Kim, N. G. Deshpande, H. W. Suh, H. H. Lee, J. H. Choi, H. S. Lee and H. K. Cho, *Adv. Funct. Mater.*, 2021, **31**, 2102439.
3. Y. Cheng, Z. Li, T. Tang, K. Xu, H. Yu, X. Tao, C. M. Hung, N. D. Hoa, Y. Fang, B. Ren, H. Chen and J. Z. Ou, *Applied Materials Today*, 2022, **26**, 101355.
4. V. Paolucci, G. D'Olimpio, C.-N. Kuo, C. S. Lue, D. W. Boukhvalov, C. Cantalini and A. Politano, 2020.
5. Y. Yang, D. Zhang, D. Wang, Z. Xu and J. Zhang, *J. Mater. Chem. A*, 2021, **9**, 14495-14506.
6. B.-R. Wang, L.-Y. Liu, G.-C. Guo, Y.-J. Bai, J.-C. Tu and R.-Z. Wang, *Appl. Surf. Sci.*, 2022, **584**, 152669.
7. H. Yang, C. Zhu, Q. Wu, X. Li, H. Wang, J. Wan, C. Xie and D. Zeng, *Appl. Surf. Sci.*, 2022, **601**, 154213.
8. S. Rani, M. Kumar, P. Garg, R. Parmar, A. Kumar, Y. Singh, V. Baloria, U. Deshpande and V. N. Singh, *ACS Appl. Mater. Interfaces*, 2022, **14**, 15381-15390.
9. S. Cui, H. Pu, E. C. Mattson, Z. Wen, J. Chang, Y. Hou, C. J. Hirschmugl and J. Chen, *Anal. Chem.*, 2014, **86**, 7516-7522.
10. G. Lee, S. Kim, S. Jung, S. Jang and J. Kim, *Sens. Actuators B Chem.*, 2017, **250**, 569-573.
11. B. Han, Z. Duan, J. Xu, Y. Zhu, Q. Xu, H. Wang, H. Tai, J. Weng and Y. Zhao, *Adv. Funct. Mater.*, 2020, **30**, 2002232.
12. A. Govind, P. Bharathi, G. Mathankumar, M. K. Mohan, J. Archana, S. Harish and M. Navaneethan, *Diamond Relat. Mater.*, 2022, **128**, 109205.
13. P. Sowti khiabani, E. Marzbanrad, H. Hassani and B. Raissi, *J. Am. Ceram. Soc.*, 2013, **96**, 2493-2498.
14. S. Shah, S. Han, S. Hussain, G. Liu, T. Shi, A. Shaheen, Z. Xu, M. Wang and G. Qiao, *Ceram. Int.*, 2022, **48**, 12291-12298.
15. S. Park, Y. W. Jung, G. M. Ko, D. Y. Jeong and C. Lee, *Applied Physics A*, 2021, **127**, 898.